

Article

Cytotoxic Polyketides from a Deep-Sea Sediment Derived Fungus *Diaporthe phaseolorum* FS431

Zheng Niu, Yuchan Chen, Heng Guo, Sai-Ni Li, Hao-Hua Li, Hong-Xin Liu, Zhaoming Liu * and Weimin Zhang * 

State Key Laboratory of Applied Microbiology Southern China, Guangdong Provincial Key Laboratory of Microbial Culture Collection and Application, Guangdong Open Laboratory of Applied Microbiology, Guangdong Institute of Microbiology, Guangdong Academy of Sciences, Yuexiu District, Guangzhou 510070, China

* Correspondence: liuzm@gdim.cn (Z.L.); wmzhang@gdim.cn (W.Z.); Tel.: +86-20-8768-8309 (W.Z.)

Received: 22 July 2019; Accepted: 21 August 2019; Published: 22 August 2019



Abstract: Two new chromone-derived polyketides phaseolorins, G and H (**1** and **2**), and one new anthraquinone derivative, phaseolorin I (**3**), together with three known compounds (**4–6**), were isolated from the deep-sea sediment-derived fungus *Diaporthe phaseolorum* FS431. The structures of the new compounds were determined by comprehensive analysis of their spectroscopic data, and the absolute configuration of **1** was established by quantum chemical calculations of electron capture detection (ECD). All the isolated compounds (**1–6**) were tested for their in vitro cytotoxic activities against four human tumor cell lines, of which compound **4** exhibited significant effect against MCF-7, HepG-2, and A549 tumor cell lines with IC₅₀ values of 2.60, 2.55, and 4.64 μM, respectively.

Keywords: *Diaporthe phaseolorum*; deep-sea derived fungus; polyketides; cytotoxicity

1. Introduction

Secondary metabolites from marine fungi have attracted the attention of chemists and biologists because of their unique chemical structures and significant biological activities [1]. In past decades, large numbers of novel chemical structures have been found from deep-sea fungi, such as polyketides, terpenoids, steroids, peptides, alkaloids, and so on [2,3]. Furthermore, polyketides have not only dominant numbers in structures but also diverse potent bioactivities, including cytotoxic, antibacterial, antifungal, radical scavenging, and antiviral [4–6].

The genus *Diaporthe* is one of the most common and widely distributed fungal taxa, which predominantly produces a large number of polyketides. Because of its importance as plant pathogen, the genus has been thoroughly investigated. Its secondary metabolites were collected from a wide range of species derived from different habitats, which were mostly obtained from endophytic fungi. Their metabolites are full of diverse natural products, such as diketopiperazines [7], triterpenoid [8], bisanthraquinones [9], highly substituted benzophenones [10], lactons [11], xanthenes [12], and mycotoxins [12], which exhibit anti-IAV [6], anti-angiogenic [7], antimalarial [12], antihyperlipidemic [13] activities, and so on.

However, the investigation of the genus *Diaporthe* from deep-sea was rarely reported. In our ongoing effort to search for bioactive metabolites from the deep-sea derived fungi, a strain of *D. phaseolorum* FS431 was collected from a sediment sample of the Indian Ocean, and its chemical investigation led to the isolation and the identification of three new polyketides, named phaseolorin G-I (**1–3**), along with three known compounds, phomoxanthone A (**4**) [14], dicerandrol B (**5**) [15], and 2,2',6'-trihydroxy-4-methyl-6-methoxy-acyl-diphenylmethanone (**6**) (Figure 1) [16]. All the isolated compounds were tested for their in vitro cytotoxic activities against four human tumor cell lines. Herein, the details of isolation, structure identification, as well as cytotoxicity assay are reported.

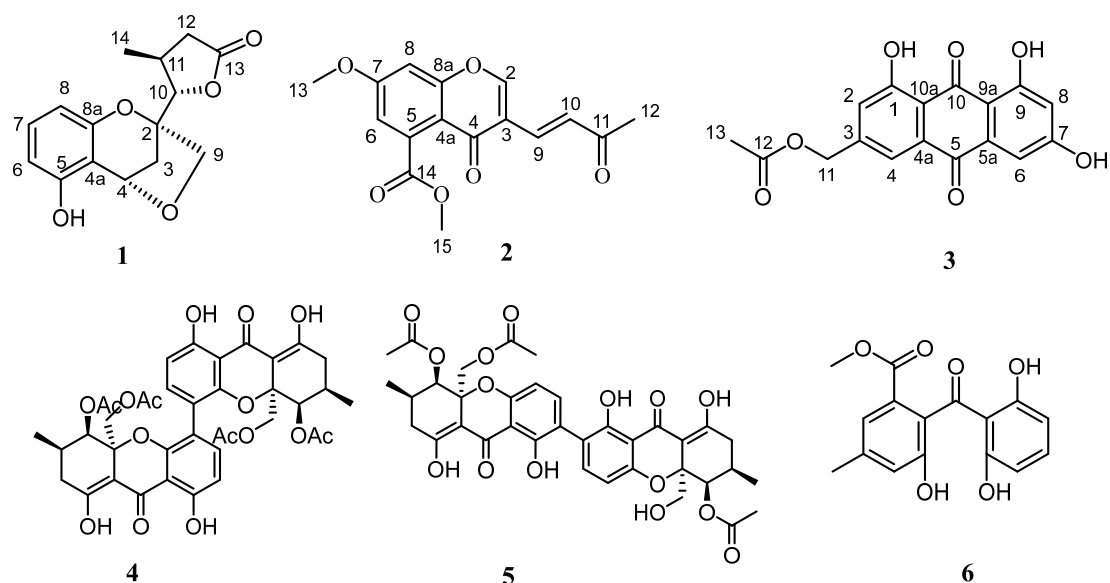


Figure 1. Chemical structures of compounds 1–6.

2. Results and Discussion

2.1. Structure Elucidation

Compound **1** was isolated as yellow oil. Its molecular formula was established to be $C_{15}H_{16}O_5$ on the basis of high-resolution electrospray ionization mass spectroscopy (HRESIMS) at m/z 275.0926 $[M - H]^-$ (calcd for 275.0919), indicating eight degrees of unsaturation. The IR absorption at 3225 and 1740 cm^{-1} suggested the presence of hydroxy and carbonyl groups, respectively. The $^1\text{H-NMR}$ spectrum of **1** revealed the presence of a phenolic hydroxyl signal at δ_{H} 8.59 (1H, br s, 1-OH), three ABX coupling aromatic protons at [δ_{H} 6.42 (1H, br d, $J = 8.1\text{ Hz}$, H-6), 6.97 (1H, t, $J = 8.1\text{ Hz}$, H-7), 6.31 (1H, br d, $J = 8.1\text{ Hz}$, H-8)], three methylenes at [δ_{H} 4.05 (2H, s, H-9), 2.22 (1H, m, H-3a), 2.12 (1H, m, H-3b), 2.85 (1H, overlapped, H-12a), 2.24 (1H, m, H-12b)], three methines at [δ_{H} 5.44 (1H, d, $J = 5.0\text{ Hz}$, H-4), 4.51 (1H, d, $J = 4.0\text{ Hz}$, H-10), 2.08 (1H, m, H-11)], and a methyl group at δ_{H} 1.28 (3H, d, $J = 6.1\text{ Hz}$, H₃-14). The $^{13}\text{C-NMR}$ combined with HSQC spectra (Table 1) of **1** resolved 15 carbon signals composed of a carbonyl carbon (δ_{C} 176.4), one methyl, three methylenes, six aromatic carbonyls, three sp^3 methines, and three aliphatic quaternary carbons. Comprehensive analysis of the 1D-NMR data indicated the existence of *thio*-trisubstituted benzene ring in **1**, which was similar to those constructed the same backbone [17].

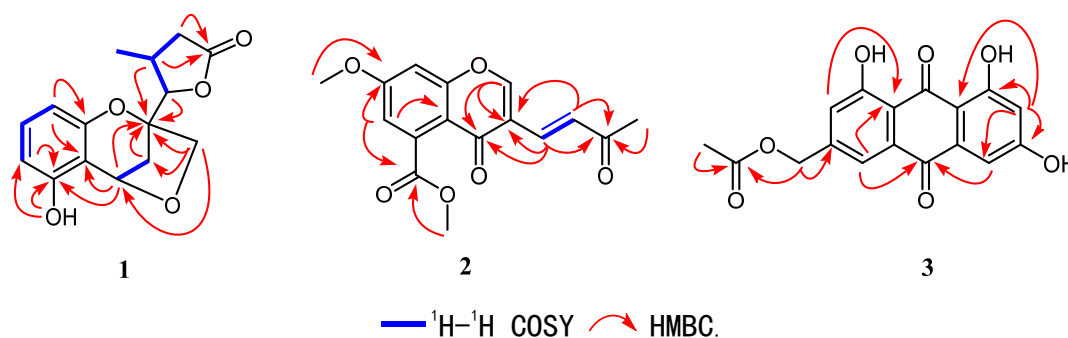
Table 1. $^1\text{H-NMR}$ (600 MHz) and $^{13}\text{C-NMR}$ (150 MHz) data for **1** in acetone- d_6 .

No.	δ_{H} (J in Hz)	δ_{C}
2		87.2, C
3a	2.22 (1H, m)	34.9, CH ₂
3b	2.14 (1H, m)	
4	5.44 (1H, d, 5.0)	69.7, CH
4a		114.2, C
5		154.8, C
6	6.42 (1H, br d, 8.0)	108.5, CH
7	6.97 (1H, t, 8.1)	130.4, CH
8	6.31 (1H, br d, 8.0)	108.2, CH
8a		155.2, C
9	4.05 (2H, s)	77.0, CH ₂
10	4.51 (1H, d, 4.0)	88.7, CH
11	2.08 (1H, m)	32.2, CH
12a	2.24 (1H, m)	
12b	2.85 (1H, overlapped)	37.4, CH ₂

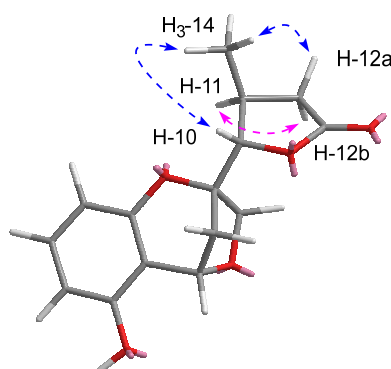
Table 1. Cont.

No.	δ_H (J in Hz)	δ_C
13		176.4, C
14	1.28 (3H, d, 6.1)	20.0, CH ₃
5-OH	8.59 (1H, br s)	

The ^1H - ^1H COSY spectrum (Figure 2) indicated the presence of four coupling fragments H-6/H-7/H-8, H-3/H-4, H-10/H-11/H-12 and H-11/H-14. The HMBC correlations (Figure 2) from H-8 to C-4a/C-8a and from H-6 to C-5/C-4a further evidenced the *thio*-trisubstituted benzene ring. Meanwhile, the correlations from H-4 to C-4a/C-5/C-8a, H-2 to C-8a, and 5-OH to C-5 suggested a benzopyran skeleton with a phenol group substituted at C-5. Moreover, the HMBC cross peaks from H₃-14 to C-10/C-12, H-11/H-12 to C-13, and H-10 to C-13 combined with the downfield shifted of H-10 and C-10 (δ_H 4.51; δ_C 88.7) further confirmed a γ -lactone ring, which was connected to C-2 on the basis of the correlation from H-10/H-11 to C-2. Finally, the correlation between H₂-9 and H-4 suggested the etherification from the hydroxymethyl to C-4, which was also supported by the degrees of unsaturation. Hence, the planar structure of **1** was established as shown in Figure 1.

Figure 2. Key ^1H - ^1H COSY and HMBC correlations for compounds 1–3.

The relative configuration between C-10 and C-11 position was deduced by the rotating overhauser effect spectroscopy (ROESY) data. The cross-peaks (Figure 3) of H-10/H₃-14/H-12a and H-11/H-12b suggested the *trans* configuration of H-10 and H-11. However, due to the lack of ROESY effects between H-4 and H₂-9, the relative configurations of C-2 and C-4 could not be identified unambiguously.

Figure 3. Key rotating overhauser effect (ROE) correlations of compound **1**.

In order to establish the complete relative configuration, the quantum chemical calculations of the NMR data of the possible diastereomers, **1a** and **1b**, were performed. Initially, an exhaustive conformation searching was conducted by Merck Molecular Force Field (MMFF) in Spartan'16 (Wavenfunction, Irvine, CA, USA). Conformers with energy less than 10 kcal mol⁻¹ energy window

were generated and reoptimized using DFT (Density Functional Theory) calculations at the b3lyp/6-31+g (d, p) level. Frequency calculations were performed at the same level to confirm that each optimized conformer was true minimum and to estimate their relative thermal free energy (ΔG) at 298.15 K.

The reoptimized conformers were further subjected to ^{13}C -NMR chemical shifts at the mPW1PW91-SCRF/6-311+G (d, p) level in acetone. The result indicated that both **1a** and **1b** shared similar correlation coefficients (R^2 : **1a** 0.9983; **1b** 0.9984, Figure 4), but the DP4⁺ (carbon data) simulation suggested **1b** should be the true candidate with 74.12% probability compared with those of **1a** (22.88% probability). Besides, **1a** exhibited a mean absolute error (MAE) value of 1.6 ppm, while **1b** showed a slightly better value of 1.5 ppm.

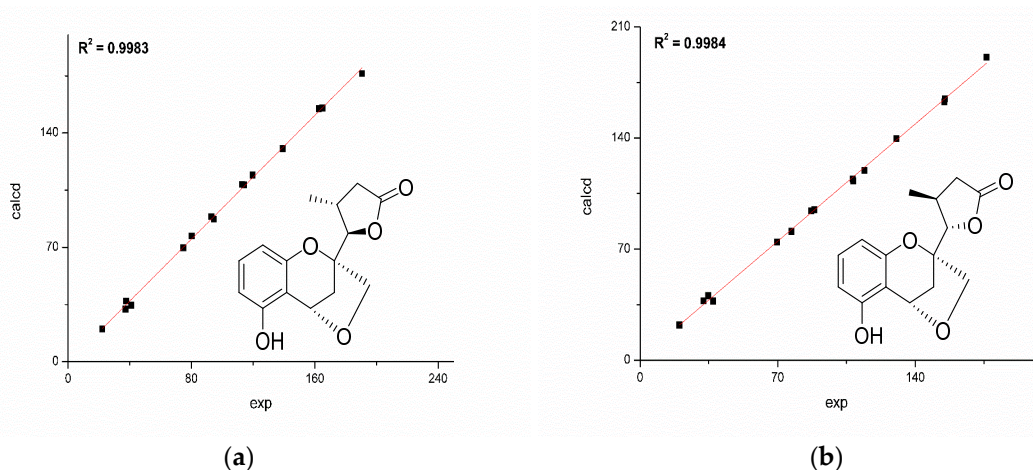


Figure 4. Correlations between experimental and calculated ^{13}C -NMR chemical shifts of **1a** (a) and **1b** (b).

Moreover, the absolute configuration could be established by the electron capture detection (ECD) calculation. The reoptimized conformers in the previous NMR calculations were selected, and the theoretical spectra of **1a/ent-1a** and **1b/ent-1b** were generated at b3lyp/6-311+g (d, p) level. The result showed that the calculated plot of *2S,4S,10S,11S-1* (**1b**) gave the best agreement with the experimental spectrum (Figure 5), which exhibited the key positive Cotton effect at 210 nm and the negative Cotton effect at 230 nm. Hence, the absolute configuration of **1** was determined to be *2S,4S,10S,11S-1*.

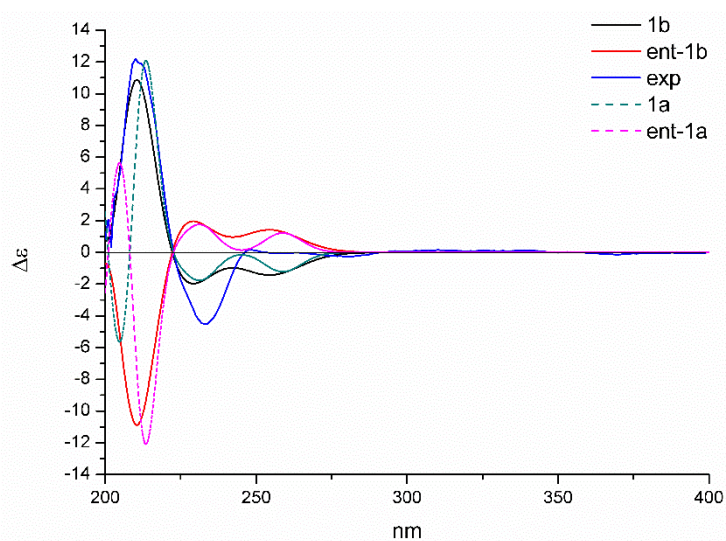


Figure 5. Calculated and experimental electron capture detection (ECD) spectra of **1** in methanol.

Compound **2** was obtained as white crystals. Its molecular formula was established to be $C_{16}H_{14}O_6$ on the basis of HRESIMS at m/z 303.0866 $[M + H]^+$ (calcd for 303.0869), indicating ten degrees of unsaturation. The UV absorption at 279 nm and IR peak at 1636 cm^{-1} suggested the existence of α , β -unsaturated carbonyl group. The $^1\text{H-NMR}$ spectrum of **2** revealed a methine group at δ_{H} 8.08 (1H, s, H-2), a double bond at [δ_{H} 7.41 (1H, d, $J = 16.1$ Hz, H-11), 7.29 (1H, d, $J = 16.1$ Hz, H-10)], two meta-coupled aromatic protons at [δ_{H} 6.96 (1H, d, $J = 2.4$ Hz, H-6), 6.92 (1H, d, $J = 2.4$ Hz, H-8)], two methoxyl signals at [δ_{H} 4.03 (3H, s, H₃-15), 3.93 (3H, s, H₃-13)], and a methyl signal at 2.35 (3H, s, H₃-12). The $^{13}\text{C-NMR}$ (Table 2) combined with HMBC spectra (Figure 2) of **2** revealed 16 carbon signals, including one methyl, two methoxyls, five sp^2 methines, and eight quaternary carbons including three carbonyl carbons at δ_{C} at 198.7, 174.2, and 169.2. By comparing the 1D-NMR data with those of diaporchromanones A–D, which were obtained as isomers from *Diaporthe phaseolorum*, compound **2** should have constructed a chromanone backbone but with a dehydrated side chain [18]. The $^1\text{H-}^1\text{H}$ COSY spectrum showed the presence of one coupling fragment, H-10/H-11. The HMBC correlations (Figure 2) from H-2 to C-3/C-4/C-8a, H-8 to C-7/C-8a, and H-6 to C-4a established the core structure of a chroman-4-one. Moreover, the HMBC cross peaks from H-6/H-15 to C-14 and H-13 to C-7 indicated a chroman-4-one skeleton, which was substituted with an ester group at C-5 and a methoxyl group at C-7. From H-9 to C-3/C-4, H-10 to C-3, a double bond was linked with C-3. Meanwhile, the geometry of the $\Delta_{9,10}$ was deduced to be *E* based on the large coupling constants ($J = 16.1$ Hz). Finally, according to the correlations from H-9/H-10/H₃-12 to C-11, an acetyl was elucidated. The above mentioned data led to the establishment of the structure of **2**.

Table 2. $^1\text{H-NMR}$ (600 MHz) and $^{13}\text{C-NMR}$ (150 MHz) data for **2** in CDCl_3 .

No.	δ_{H} (J in Hz)	δ_{C}
2	8.08 (1H, s)	156.5, CH
3		119.6, C
4		174.2, C
4a		114.8, C
5		135.3, C
6	6.96 (1H, d, 2.4)	113.9, CH
7		163.2, C
8	6.92 (1H, d, 2.4)	101.8, CH
8a		157.3, C
9	7.29 (1H, d, 16.1)	133.0, CH
10	7.41 (1H, d, 16.1)	129.7, CH
11		198.7, C
12	2.35 (3H, s)	28.6, CH ₃
13	3.93 (3H, s)	56.2, CH ₃
14		169.2, C
15	4.03 (3H, s)	53.2, CH ₃

Compound **3** was isolated as a yellow oil. Its molecular formula was established to be $C_{17}H_{12}O_7$ on the basis of HRESIMS at m/z 327.0514 $[M - H]^-$ (calcd for 327.0504), indicating twelve degrees of unsaturation. UV spectrum exhibited an obvious absorption band at 434 nm, indicating a large conjugated system in **3**. The $^1\text{H-NMR}$ spectrum (Table 3) of **3** revealed two phenol signals at [δ_{H} 12.12 (1H, br s, 1-OH), 12.12 (1H, br s, 9-OH)], an aromatic ring system present at [δ_{H} 7.63 (1H, br s, H-2), 7.31 (1H, br s, H-4)], and [δ_{H} 7.12 (1H, d, $J = 2.4$ Hz, H-6), 6.58 (1H, d, $J = 2.4$ Hz, H-8)], and one methyl signal at δ_{H} 2.14 (3H, s, H-13). The $^{13}\text{C-NMR}$ (Table 3) and the HMBC spectra (Figure 2) of **3** revealed 17 carbon signals, one methyl, one sp^3 methylenes, four sp^2 methines, and eleven quaternary carbons including three carbonyl carbons at δ_{C} 189.4, 181.3, and 170.2. The key HMBC ^3J correlations from H-4, H-6 to C-5, H-2/H-4 to C-10a, H-8 to C-6/C-9a along with weak ^4J signal from H-4 to C-10 helped define the central anthracene-9,10-dione ring. The relations from H-11 to C-3/C-12 and H₃-13 to C-12 established the fragment of methyl acetate at C-3. Moreover, the characteristic downfield chemical shifts of 1-OH and 9-OH (δ_{H} 12.12 ppm) suggested the substituted location at C-1 and C-9, forming hydrogen bonds with the carbonyl carbon (C-10).

Table 3. ^1H -NMR (600 MHz) and ^{13}C -NMR (150 MHz) data for **3** in $\text{DMSO-}d_6$.

Position	δ_{H} (J in Hz)	δ_{C}
1		161.3, C
2	7.30 (1H, br s)	122.3, CH
3		145.6, C
4	7.63 (1H, br s)	117.8, CH
4a		133.3, C
5		181.3, C
5a		135.1, C
6	7.12 (1H, br d, 2.4)	109.2, CH
7		166.2, C
8	6.58 (1H, br d, 2.4)	108.0, CH
9		164.6, C
9a		108.9, C
10		189.4, C
10a		115.1, C
11	5.18 (2H, s)	64.2, CH_2
12		170.2, C
13	2.14 (3H, s)	20.6, CH_3
1-OH	12.12 (1H, br s)	161.3, C
9-OH	12.12 (1H, br s)	

2.2. Cytotoxicity Activity

Compounds **1–6** were evaluated for their cytotoxicities against four human cancer cell lines: SF-268, MCF-7, HepG-2, and A549. Compound **4** was found to exhibit significant effects against MCF-7, HepG-2, and A549, with IC_{50} values of 2.60, 2.55, and 4.64 μM , respectively (Table 4).

Table 4. IC_{50} (μM) of compounds **4–5** against four tumor cell lines.

NO.	SF-268	MCF-7	HepG-2	A549
4	37.86 \pm 1.28	2.60 \pm 0.28	2.55 \pm 0.06	4.64 \pm 0.30
5	45.26 \pm 3.18	48.08 \pm 1.55	49.58 \pm 0.45	38.64 \pm 1.42
doxorubicin	0.57 \pm 0.04	0.95 \pm 0.06	1.18 \pm 0.15	0.70 \pm 0.04

3. Materials and Methods

3.1. General Experimental Procedures

UV spectra were recorded on a Shimadzu UV-2600 spectrophotometer (Shimadzu, Kyoto, Japan). IR data were acquired on a Shimadzu IR Affinity-1 spectrometer (Shimadzu, Kyoto, Japan). 1D- and 2D-NMR spectra were obtained on a Bruker AVANCE IIIITM HD 600 MHz NMR spectrometer (Bruker, Fällanden, Switzerland) using TMS as an internal standard. HRESIMS and electrospray ionization-mass spectrometry (ESIMS) data were measured, respectively, on a Thermo MAT95XP high resolution mass spectrometer (Thermo Fisher Scientific, Bremen, Germany) and an Agilent Technologies 1290-6430A Triple Quad LC/MS (Agilent Technologies, Palo Alto, CA, USA). Optical rotations were obtained on an Anton Paar MCP-500 spectropolarimeter (Anton Paar, Graz, Austria) with MeOH as solvent at 25 °C. CD spectra were determined using a Jasco 820 spectropolarimeter (Jasco Corporation, Kyoto, Japan). Preparative HPLC collection used a C_{18} column (YMC-pack ODS-A, 250 \times 20 mm, 5 μm , 12 nm, YMC Co., Ltd., Kyoto, Japan). Semipreparative HPLC separations were performed utilizing a C_{18} column (YMC-pack ODS-A/AQ, 250 \times 10 mm, 5 μm , 12 nm, YMC CO., Ltd., Kyoto, Japan). Column chromatography (CC) was performed on silica gel (200–300 mesh, Qingdao Marine Chemical Inc., Qingdao, China) and Sephadex LH-20 (Amersham Biosciences, Uppsala, Sweden). Solvents for isolation were analytical grade (Guangzhou Chemical Regents Company, Ltd., Guangzhou, China). TLC spots were visualized under UV light and by dipping into 10% H_2SO_4 in alcohol followed by heating.

3.2. Fungal Material

The fungal strain FS431 was isolated from a marine sediment sample collected from the Indian Ocean (depth 3605 m, 7°57.75944' N, 89°19.43851' E) in March 2016 and identified as

Diaporthe phaseolorum based on sequencing of the internal transcribed spacer (ITS) region (Accession No. MK459544) with 99% similarity to *Diaporthe phaseolorum* MJ14 (Accession No. KM203581). The strain was deposited at the Guangdong Provincial Key Laboratory of Microbial Culture Collection and Application, Guangdong Institute of Microbiology.

3.3. Fermentation and Extraction

D. phaseolorum FS431 was cultured for 5 days at 28 °C in a potato dextrose agar (PDA) culture plate. The mycelial plugs were transferred to ten 500 mL Erlenmeyer flasks, each containing 250 mL potato dextrose broth (20% potato, 2% glucose, 0.3% KH₂PO₄, 0.15% MgSO₄·7H₂O, and 250 mL water with 1.5% sea salt), and then incubated on a rotary shaker at 120 r/m and 28 °C for 4 days as seed cultures. After that, each of the seed cultures (20 mL) was transferred into autoclaved 3 L Erlenmeyer flasks (total of 10 bottles), each containing 480 g of rice and 600 mL of 3% saline water. All flasks were incubated statically at room temperature for 30 days.

3.4. Isolation and Purification

The fermented rice substrate was extracted three times with ethyl acetate (EtOAc), and the combined EtOAc layers were evaporated to dryness under vacuum to afford the EtOAc extract (122.7 g). The EtOAc extract was chromatographed on a silica gel (200–300 mesh) column eluted with a step gradient of petroleum ether (PE)–EtOAc (*v/v* 30:1, 20:1, 10:1, 5:1, 2:1, 1:1, 0:1) and CH₂Cl₂–MeOH (*v/v* 20:1, 10:1, 5:1) to give 10 fractions (Fr. 1–Fr. 10). Fr. 6 was chromatographed by ODS column chromatography using gradient elution of H₂O–MeOH (30–100%) to give 7 subfractions (Fr. 6.1–Fr. 6.7). Fr. 6.3 was purified by silica gel flash column chromatography (PE/EtOAc *v/v* 10:1–2:1) to yield 4 fractions (Fr. 6.3.1–Fr. 6.3.4). Fr. 6.3.4 was subjected to CC on Sephadex LH-20 (CH₂Cl₂/MeOH *v/v*, 1:1), and semiprep-HPLC (MeOH/H₂O *v/v*, 50:50, 3 mL/min) to give compound 1 (3.3 mg, *t_R* = 9.2 min) and 6 (10.5 mg, *t_R* = 11.8 min). Fr. 6.6 was purified by silica gel flash column chromatography (PE/CH₂Cl₂ *v/v* 5:1–1:1) to yield 4 fractions (Fr. 6.6.1–Fr. 6.6.4). Fr. 6.6.2 was purified by Sephadex LH-20 (CH₂Cl₂/MeOH, 1:1, *v/v*) to yield compound 3 (5.3 mg). Fr. 6.6.4 was purified by Sephadex LH-20 (CH₂Cl₂/MeOH, 1:1, *v/v*) to yield 2 fractions (Fr. 6.6.4.1–Fr. 6.6.4.2), and Fr. 6.6.4.1 was further purified by semiprep-HPLC (MeOH/H₂O *v/v* 60:40, 3 mL/min) to yield compound 2 (3.2 mg, *t_R* = 20.5 min). Fr. 6.6.4.2 was purified by semiprep-HPLC (MeOH/H₂O, 70:30, *v/v*, 3 mL/min) to yield compound 7 (3.2 mg, *t_R* = 13 min). Fr. 6.7 was purified by silica gel flash column chromatography (PE/CH₂Cl₂ *v/v* 20:1–5:1) to yield (Fr. 6.7.1–Fr. 6.7.2). Fr. 6.7.2 was then purified by semiprep-HPLC (MeOH/H₂O *v/v* 90:10, 3 mL/min) to yield compound 4 (23.0 mg, *t_R* = 6.3 min) and compound 5 (7.4 mg, *t_R* = 7.3 min).

3.5. Quantum Chemical Calculation of NMR Chemical Shifts and ECD Spectra

MMFF and DFT/TD-DFT calculations were carried out using the Spartan'14 software (Wavefunction Inc., Irvine, CA, USA) and the Gaussian 09 program, respectively. Conformers that had an energy window lower the 5 kcal·mol⁻¹ were generated and optimized using DFT calculations at the b3lyp/6-31+g (d, p) level. Frequency calculations were performed at the same level to confirm that each optimized conformer was true minimum and to estimate their relative thermal free energy (ΔG) at 298.15 K. Conformers with the Boltzmann distribution over 2% were chosen for ¹³C-NMR and ECD calculations at mPW1PW91/6-311+g (d, p) and b3lyp/6-311+g (d, p) level, respectively. Additionally, solvent effects were considered based on the self-consistent reaction field (SCRF) method with the polarizable continuum model (PCM). Details of the conformers' information were provided in Supporting Information. The ECD spectrum was generated by the SpecDis program using a Gaussian band shape with 0.22 eV exponential half-width from dipole-length dipolar and rotational strengths. The DP4⁺ probability simulations were conducted using an applet available at <http://www-jmg.ch.cam.ac.uk/tools/nmr/DP4/>.

3.6. Cytotoxic Activity Assay

Cytotoxicity of compounds (1–6) were assayed against four tumor cell lines, including SF-268 (human glioma cell line), MCF-7 (human breast adenocarcinoma cell line), HepG-2 (human liver cell line), and A549 (human lung cancer cell line). Assays were performed by the SRB method [19] with doxorubicin as the positive control. Cells (180 μ L) with a density of 30,000 cells/mL of media were injected into 96-well plates and incubated at 37 °C for 24 h under 5% CO₂. Then, tested compounds (20 μ L) were added. After incubating for 72 h, cell monolayers were fixed with 50 μ L trichloroacetic acid (*w/v*: 50%) and stained with 0.4% SRB (dissolved in 1% acetic acid) for 30 min. The monolayers were washed by 1% acetic acid three times to remove the unbound dye. Finally, the mixtures were dissolved in 200 μ L Tris base solution (10 mM) and recorded the OD at 570 nm using a microplate reader. All data were obtained in triplicate.

3.7. Spectroscopic Data

Phaseolorin G (1): Yellow powder, $[\alpha]_D^{25} = +35.4$ (c 0.08, MeOH); UV (MeOH) λ_{\max} (log ϵ) 205 (3.49), 278 (2.28) nm; CD $\Delta\epsilon$ (0.18 mg/mL, MeOH) λ_{\max} ($\Delta\epsilon$) 210 (+12.2), 233 (-4.5), 248 (+0.2) nm; IR (KBr) ν_{\max} 3225, 2924, 1740, 1260 cm^{-1} ; ¹H- and ¹³C-NMR data, see Table 1 and Supplementary Materials; (–)-HRESIMS *m/z* 275.0926 [M – H][–] (calcd for C₁₅H₁₅O₅ 275.0919).

Phaseolorin H (2): White crystals, m.p. 289–291 °C; λ_{\max} (log ϵ) 207 (3.62), 279 (3.21) nm; IR (KBr) ν_{\max} 3225, 2920, 1636, 1260 cm^{-1} ; ¹H- and ¹³C-NMR data, see Table 2 and Supplementary Materials; (+)-*m/z* 303.0866 [M + H]⁺ (calcd for C₁₆H₁₅O₆ 303.0869).

Phaseolorin I (3): Yellow oil, λ_{\max} (log ϵ) 222 (3.14), 265 (2.82), 286 (2.83), 434 (2.61) nm; IR (KBr) ν_{\max} 3300, 2922, 1609, 1260 cm^{-1} ; ¹H- and ¹³C-NMR data, see Table 3 and Supplementary Materials; (–)-HRESIMS *m/z* 327.0514 [M – H][–] (calcd for C₁₇H₁₁O₇ 327.0504).

4. Conclusions

The chemical investigation of the deep-sea derived fungus *D. phaseolorum* FS431 led to isolation of three new polyketides, named phaseolorin G–I (1–3), together with three known compounds (4–6). Their structures were elucidated by the detailed analysis of spectroscopic data and quantum chemical calculations. Compound 4 exhibited significant cytotoxic activities against MCF-7, HepG-2, and A549 cancer cell lines with IC₅₀ values of 2.60, 2.55, and 4.64 μ M, respectively. This study makes a contribution to the chemical diversities of polyketides from deep-sea derived fungi.

Supplementary Materials: The Supplementary Materials are available online. Figures S1–S24: HRESIMS, CD, UV, IR, 1D- and 2D-NMR spectra of compounds 1–3; Figures S25–S30: 1D-NMR spectra of compounds 4–6.

Author Contributions: Data curation, Z.L., Z.N.; Formal analysis, Z.L., H.-X.L.; Funding Acquisition, W.Z.; Investigation, Z.N., Z.L., Y.-C.C., and H.-H.L.; Project Administration, W.Z.; Resources, H.G. and S.-N.L.; Writing—Original Draft, Z.N.; Writing—Review & Editing, Z.L. and W.Z.; Supervision, Z.L. and W.Z.

Funding: This work was supported financially by the National Natural Science Foundation of China (41906106), Science and Technology Program of Guangzhou, China (201607020018), the Team Project of the Natural Science Foundation of Guangdong Province (2016A030312014), and the GDAS' Project of Science and Technology Development (2019GDASYL-0103007).

Conflicts of Interest: The authors declare no conflicts of interest.

References

1. Bugni, T.S.; Ireland, C.M. Marine-derived fungi: A chemically and biologically diverse group of microorganisms. *Nat. Prod. Rep.* **2004**, *21*, 143–163. [[CrossRef](#)] [[PubMed](#)]
2. Rateb, M.E.; Ebel, R. Secondary metabolites of fungi from marine habitats. *Nat. Prod. Rep.* **2011**, *28*, 290. [[CrossRef](#)] [[PubMed](#)]
3. Skropeta, D.; Wei, L. Recent advances in deep-sea natural products. *Nat. Prod. Rep.* **2014**, *31*, 999–1025. [[CrossRef](#)] [[PubMed](#)]

4. Wang, W.; Liao, Y.; Zhang, B.; Gao, M.; Ke, W.; Li, F.; Shao, Z. Citrinin Monomer and Dimer Derivatives with Antibacterial and Cytotoxic Activities Isolated from the Deep Sea-Derived Fungus *Penicillium citrinum* NLG-S01-P1. *Mar. Drugs* **2019**, *17*, 46. [[CrossRef](#)] [[PubMed](#)]
5. Pang, X.; Lin, X.; Yang, J.; Zhou, X.; Yang, B.; Wang, J.; Liu, Y. Spiro-Phthalides and Isocoumarins Isolated from the Marine-Sponge-Derived Fungus *Setosphaeria* sp. SCSIO41009. *J. Nat. Prod.* **2018**, *81*, 1860–1868. [[CrossRef](#)] [[PubMed](#)]
6. Luo, X.W.; Yang, J.; Chen, F.M.; Lin, X.P.; Chen, C.M.; Zhou, X.F.; Liu, S.W.; Liu, Y.H. Structurally diverse polyketides from the mangrove-derived fungus *Diaporthe* sp. SCOSIC 41011 with their anti-influenza A virus activities. *Front. Chem.* **2018**, *6*, 1–10. [[CrossRef](#)] [[PubMed](#)]
7. Chang, F.-R.; Wang, S.-W.; Li, C.-Y.; Lu, Y.-Y.; Liu, S.-Y.V.; Chen, C.-Y.; Wu, Y.-C.; Cheng, Y.-B. Natural Products from *Diaporthe* arecae with Anti-Angiogenic Activity. *Isr. J. Chem.* **2019**, *59*, 439–445. [[CrossRef](#)]
8. Li, G.; Kusari, S.; Kusari, P.; Kayser, O.; Spiteller, M. Endophytic *Diaporthe* sp. LG23 produces a potent antibacterial tetracyclic triterpenoid. *J. Nat. Prod.* **2015**, *78*, 2128–2132. [[CrossRef](#)] [[PubMed](#)]
9. Tian, W.; Liao, Z.; Zhou, M.; Wang, G.; Wu, Y.; Gao, S.; Qiu, D.; Liu, X.; Lin, T.; Chen, H. Cytoskyrin C, an unusual asymmetric bisanthraquinone with cage-like skeleton from the endophytic fungus *Diaporthe* sp. *Fitoterapia* **2018**, *128*, 253–257. [[CrossRef](#)] [[PubMed](#)]
10. Zhang, C.W.; Ondeyka, J.G.; Herath, K.B.; Guan, Z.Q.; Collado, J.; Platas, G.; Pelaez, F.; Leavitt, P.S.; Gurnett, A.; Nare, B.; et al. Tenellones A and B from a *Diaporthe* sp.: Two highly substituted benzophenone inhibitors of parasite cGMP-dependent protein kinase activity. *J. Nat. Prod.* **2005**, *68*, 611–613. [[CrossRef](#)] [[PubMed](#)]
11. Brady, S.F.; Wagenaar, M.M.; Singh, M.P.; Janso, J.E.; Clardy, J. The Cytosporones, New Octaketide Antibiotics Isolated from an Endophytic Fungus. *Org. Lett.* **2000**, *2*, 4043–4046. [[CrossRef](#)] [[PubMed](#)]
12. Calcul, L.; Waterman, C.; Ma, W.S.; Lebar, M.D.; Harter, C.; Mutka, T.; Morton, L.; Maignan, P.; Olphen, A.; Kyle, D.E.; et al. Screening Mangrove Endophytic Fungi for Antimalarial Natural Products. *Mar. Drugs* **2013**, *11*, 5036–5050. [[CrossRef](#)] [[PubMed](#)]
13. Hu, M.; Yang, X.Q.; Wan, C.P.; Wang, B.Y.; Yin, H.Y.; Shi, L.J.; Wu, Y.M.; Yang, Y.B.; Zhou, H.; Ding, Z.T. Potential antihyperlipidemic polyketones from endophytic *Diaporthe* sp. JC-J7 in *Dendrobium nobile*. *RSC Adv.* **2018**, *8*, 41810–41817. [[CrossRef](#)]
14. Isaka, M.; Jaturapat, A.; Rukseree, K.; Danwisetkanjana, K.; Tanticharoen, M.; Thebtaranonth, Y. Phomoxanthonones A and B, Novel Xanthone Dimers from the Endophytic Fungus *Phomopsis* Species. *J. Nat. Prod.* **2001**, *64*, 1015–1018. [[CrossRef](#)] [[PubMed](#)]
15. Wagenaar, M.M.; Clardy, J. Dicerandrols, new antibiotic and cytotoxic dimers produced by the fungus *Phomopsis longicolla* isolated from an endangered mint. *J. Nat. Prod.* **2001**, *64*, 1006–1009. [[CrossRef](#)] [[PubMed](#)]
16. Zhang, L.-H.; He, F.-J.; Hua, H.-M.; Liu, B.; Wang, H.-F.; Liu, F.; Bai, J.; Chen, G.; Pei, Y.-H. Isolation of a New Compound from *Penicillium oxalicum*. *Chem. Nat. Compd.* **2016**, *52*, 821–823.
17. Guo, H.; Liu, Z.-M.; Chen, Y.-C.; Tan, H.-B.; Li, S.-N.; Li, H.-H.; Gao, X.-X.; Liu, H.-X.; Zhang, W.-M. Chromone-Derived Polyketides from the Deep-Sea Fungus *Diaporthe phaseolorum* FS431. *Mar. Drugs* **2019**, *17*, 182. [[CrossRef](#)] [[PubMed](#)]
18. Cui, H.; Liu, Y.N.; Li, J.; Huang, X.S.; Yan, T.; Cao, W.H.; Liu, H.J.; Long, Y.H.; She, Z.G. Diaporindenes A–D: Four unusual 2,3-dihydro-1H-indene analogues with anti-inflammatory activities from the mangrove endophytic fungus *Diaporthe* sp. SYSU-HQ3. *J. Org. Chem.* **2018**, *83*, 11804–11813. [[CrossRef](#)] [[PubMed](#)]
19. Skehan, P.; Scudiero, D.; Vistica, D.; Bokesch, H.; Kenney, S.; Storeng, R.; Monks, A.; McMahon, J.; Warren, J.T.; Boyd, M.R. New Colorimetric Cytotoxicity Assay for Anticancer-Drug Screening. *J. Natl. Cancer Inst.* **1990**, *82*, 1107–1112. [[CrossRef](#)] [[PubMed](#)]

Sample Availability: Samples of the compounds 1–6 are available from the authors.



© 2019 by the authors. Licensee MDPI, Basel, Switzerland. This article is an open access article distributed under the terms and conditions of the Creative Commons Attribution (CC BY) license (<http://creativecommons.org/licenses/by/4.0/>).